JVSTB

Journal of Vacuum Science & Technology B | 2nd Series | Volume 41, Number 3 | May/June 2023

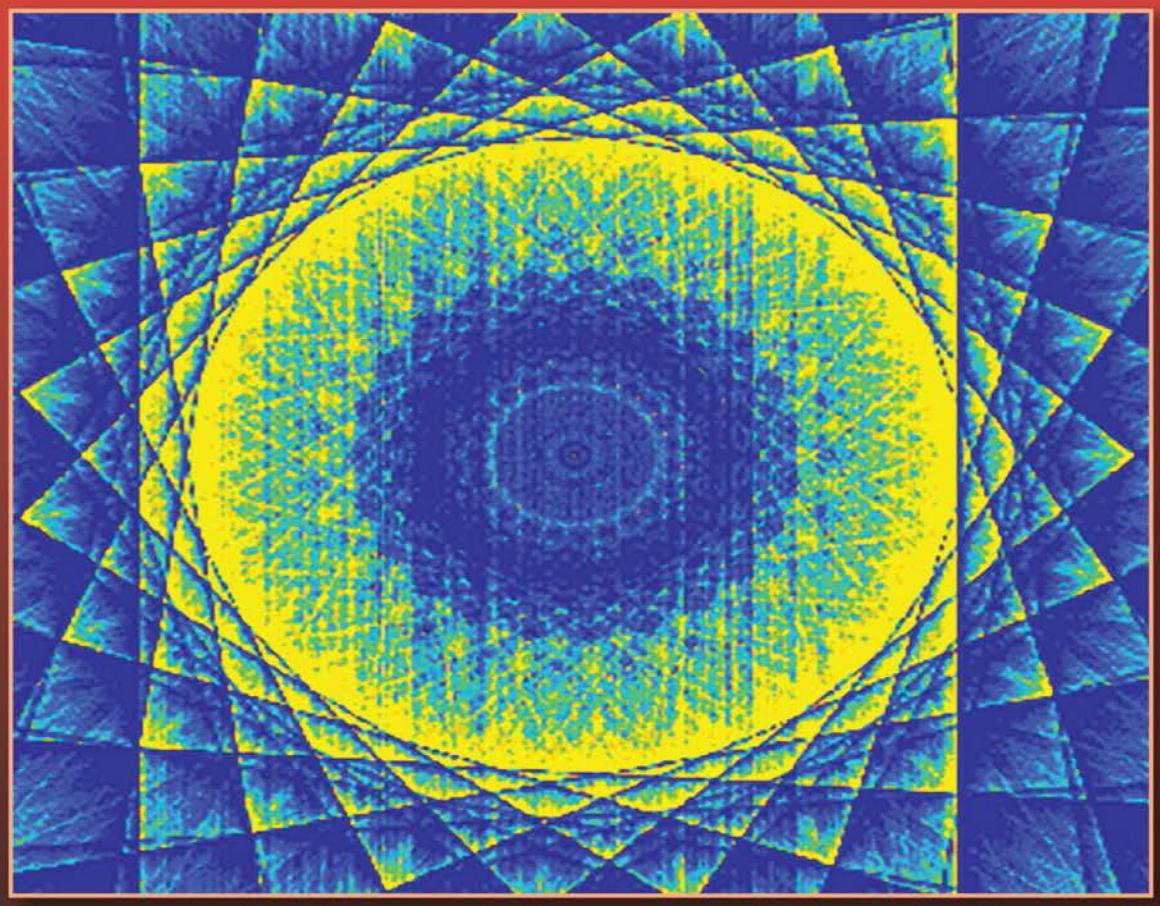

Image Credit: Jaydip Sawant, Yi Yin Yu, Ketan Bhotkar, Hyun-Jung Jung, Gi Joon Nam, and Kyu Chang Park, JVST B 41 (3), 10.1116/6.0002286, (2023).

Review Articles

An AVS journal published by the Society through AIP Publishing LLC

JVST B
Journal of Vacuum Science & Technology B

REVIEW

avs.scitation.org/journal/jvb

Secondary ion mass spectrometry quantification: Do you remember when a factor of 2 was good enough?

Cite as: J. Vac. Sci. Technol. B **41**, 030803 (2023); doi: 10.1116/6.0002466
Submitted: 30 December 2022 · Accepted: 20 March 2023 ·
Published Online: 20 April 2023

Charles W. Magee[1,a)] and Temel H. Buyuklimanli[2,b)]

AFFILIATIONS

[1]Eurofins EAG Laboratories, 104 Windsor Center Drive, Suite 101, East Windsor, New Jersey 08520
[2]Eurofins EAG Laboratories, 810 Kifer Road, Sunnyvale, California 94086

Note: This paper is part of the 2023 Special Topic Collection on Secondary Ion Mass Spectrometry (SIMS).
[a)]**Electronic mail:**charlesmagee@eurofinseag.com
[b)]**Electronic mail:** temel@eurofinseag.com

ABSTRACT

Well, do you remember when a factor of 2 was good enough? Probably, not unless you have been around secondary ion mass spectrometry (SIMS) since the early 1960s, like one of us has been. This paper will give many references back to the early days of quantification when a local thermal equilibrium model was used to obtain the first results that were accurate to within a factor of 2, but only 60% of the time. It only worked for bulk silicate matrixes. People were not even using SIMS on semiconductors in those days. Several early references showing profiles of ion implants in Si will be referenced, but it was not until 1980 that the first paper was published that explicitly showed how to use ion implants as SIMS standards. People were using ion implants as standards before 1980, but only in limited cases, and with no formal published equations specifying how to use them. But, the samples for which ion implants were used as standards were for dilute concentrations in a single matrix, which had a uniform matrix composition with depth. The rest of the paper will show how we at Eurofins EAG Laboratories tackled the problem of quantification of both major and minor elements in nonuniform, multi-element matrices with continuously graded composition changes using point-by-point CORrected-SIMS. These include SiGe heterostructure bipolar transistors, AlGaAs vertical cavity surface emitting lasers, and B plasma-implanted poly-silicon gates.

I. INTRODUCTION

"Modern-day" secondary ion mass spectrometry dates back to a 1958 paper by R. E. Honig of RCA Laboratories.[1] He sputtered Ge and SiGe with 400 eV inert gas ions. (See later figures…he was 40 years ahead of his time looking at SiGe!) The same work was presented at a conference. In those proceedings,[2] questions asked after the presentation were published along with Honig's answers. His last answer is particularly interesting when viewed today.

Q: "What are the possibilities of this type of ion source for analytical work?"
A: "At the present time, I am rather pessimistic. The difficulties involved in producing secondary particles by sputtering are such that, so far, I would not think it possible to make impurity determinations beyond, say, one part in 1000. However, it is possible that this might improve in the future."

And indeed, it did… by a factor of 10 000 000!

The path forward[3] for this improvement in detection limits is shown in Fig. 1, made a decade after Honig's pessimistic pronouncement.

Positive secondary ions are formed in the collision cascade and escape the surface before being neutralized by electrons from the surface. The survival rate of the leaving ions is a function of the electronic properties of the surface. The survival rate of the ions can be much improved by controlling the chemistry of the surface through bombardment with reactive gases. In 1969, C. A. Anderson of Applied Research Laboratories showed that instead of

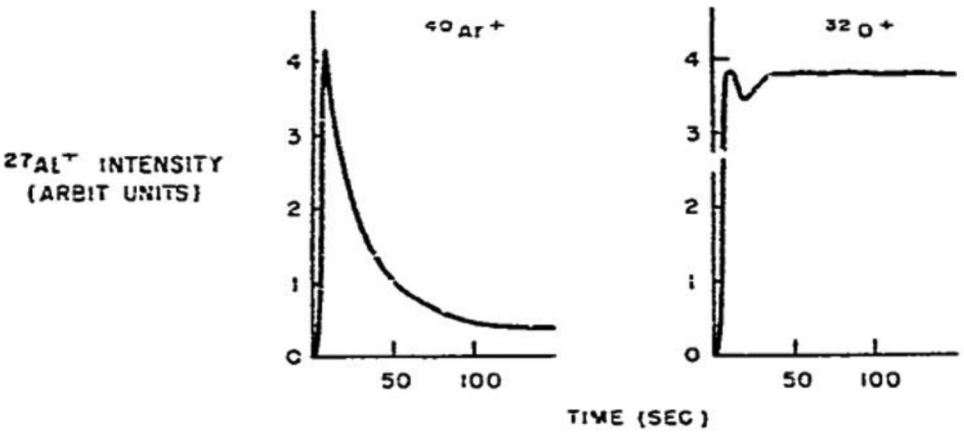

FIG. 1. Variation with time of the sputtered positive ion intensity from pure Al under bombardment with an inert gas, Ar^+, and with an electronegative species, O_2^+. The primary ion accelerating potential is 11 kV. [Reprinted from C.A. Andersen, Int. J. Mass Spectrom. Ion Phys. **2**, 61 (1969). Copyright 1969, with permission from Elsevier.].

bombarding with inert gas ions, if one bombarded with oxygen ions, positive secondary ion intensity could be made to reach a stable, much higher level than was possible using argon bombardment[3] as shown in Fig. 1. Oxygen bombardment then came to dominate the way positive secondary ions were generated. In the same paper, Andersen also showed that negative ion sensitivity could be enhanced by sputtering with Cs ions instead of Xe ions,[3] which initially was reported by Victor Krohn.[4]

II. EARLY METHODS OF QUANTIFICATION

A. Working-curve approach

In the same publication,[3] Anderson showed how SIMS could use the traditional approach in analytical chemistry for quantification, than using a series of standards to develop a working curve of detected signal vs impurity concentration. The paper showed how the sensitivity of low levels (<0.8%) of Mg in Al behaved ideally in that the intensity of detected secondary ions depended linearly on the Mg concentration.

But another plot in that paper showed a significant problem with SIMS that has made major (matrix-level) elements difficult to quantify. The data showed that for concentrations of Fe in Al in the 1%–7% range, the relationship between the detected signal intensity and concentration was no longer linear. That is, the presence of an element at a high concentration affected that element's own sensitivity. This would prove to be a major stumbling block to using SIMS for major element quantification, but as we will show, not an insurmountable one.

B. First principal approach to quantification (the LTE model)

In 1973[5,6] and 1975,[7] C. A. Andersen tried to quantify secondary ion intensities by calculating the ratio of sputtered positive ions to sputtered neutral atoms using the Saha–Eggert ionization equation, assuming a plasma is formed in local thermal equilibrium (LTE) during the sputtering process:

$$\log_e (n^+/n^0) = 15.4 + 1.5 \log_e T + \log_e (2B^+/B^0) - \frac{5040}{T}(I_p - \Delta E) - \log_e n^-, \quad (1)$$

where n^+ = number density of positive ions, n^0 = number density of neutral atoms, T = temperature in degrees K, B = internal partition function, I_p = first ionization potential, ΔE = depression of the ionization potential, and n^- = density of free electrons. All the above were available in tables or could be calculated except for the plasma temperature and the density of free electrons. However, these two quantities could be determined experimentally if two impurities were present in known concentrations in the analytical sample. Andersen called this his LTE model.

In 1978, D.E. Newbury[8] showed that the LTE method, while the best method available at the time for quantification, had some significant deficiencies. He found that for over 100 determinations on a wide range of elements in a series of NIST (National Institute for Standards and Technology) glass samples, only 53% of the unknown values came within a factor of 2 of the accepted values. Eighty-four percent of the determinations were within a factor of 5, and 14% were in error by more than a factor of 5. Newbury then compared the LTE approach with the working-curve approach using standards. Using this traditional (albeit very time-consuming) approach, 83% of the unknown values came with a factor of 2 of the accepted values, and 99% of the determinations were within a factor of 5. No determinations were in error by more than a factor of 5. The degree of accuracy of the LTE model was deemed a success in the 1970s because it was all that was generally available.

C. Quantification using standards

Even though the NIST study clearly showed that using standards and the working-curve approach was more accurate than the LTE model, there were no widely available standards for SIMS for semiconductor materials in the 1970s. NIST had many multi-element standards in glasses and metals that were used in this time period, but they were made for bulk-analysis techniques and not certified for microhomogeneity, which is needed for a SIMS standard. It was imperative to have standards for SIMS because of the great

variability of elemental sensitivities across the periodic table as first seen by Anderson[3] and later measured more completely by Storms.[9]

That is not to say that accurate SIMS profiles were not being made by this time. A seminal paper by the Philips Research group in 1975[10] showed ion-implanted B profiles over a wide range of energies. But, these early B implants were not meant to be standards. They were to investigate the exact shape of ion-implanted distributions because, at that time, the exact profile shapes were not known.[11]

It was not until 1980 that the first paper was published showing how ion implantation could be used to fabricate SIMS standards by introducing known amounts of virtually any element into a variety of semiconductor matrices.[12] Knowledge of the implanted dose and accurate depth data could be used to convert raw secondary ion signal vs sputter time into concentration vs depth data. (It is noted in Ref. 12 that this method of integration of the total number of detected ions made prior knowledge of the implant shape unnecessary. Theoretical profile shapes were not needed, and ion channeling of the implant made no difference in the accuracy of calculations.) This allowed one to determine sensitivity factors for any implanted element in virtually any matrix. These relative sensitivity factors (RSFs) could then be used to quantify the unknown amounts of those elements in the matrix of the standard using the equation:

$$\rho_i = \frac{I_i}{I_m} \mathrm{RSF}, \tag{2}$$

where ρ_i is the impurity concentration in atoms/cm^3, I_i is the impurity isotope secondary ion intensity in counts/s, I_m is the matrix isotope secondary ion intensity in counts/s, and RSF has units of atoms/cm^3. This proved useful (and continues to be useful, today) for dilute concentration (<2%–4% atomic) in a single matrix, i.e., no layers of a different matrix.

However, by the early 1990s, devices were being fabricated with heterostructures. The SiGe heterostructure bipolar transistor (HBT) is a prime example. The target structure for such a device is shown in Fig. 2.

The collector of the device is pure Si. The base is fabricated (by MOCVD) with an abrupt increase in the Ge content followed by a gradual decrease in [Ge] until the emitter is grown, again with pure Si. The base layer is grown with a B-doped layer centered in the graded SiGe layer. If the B was present in a SiGe layer with a constant [Ge], then one could use a standard of B ion implanted into a SiGe layer of the same Ge concentration, [Ge], as that of the SiGe layer in the HBT. The B profile for the entire structure could then be "stitched together" with a B RSF in Si for the emitter and the collector, and a B RSF in SiGe for the base layer. But, that will not work for a graded [Ge]. One would expect the B sensitivity to change continuously with the changing Ge concentration.

III. MODERN METHODS OF QUANTIFICATION NEEDED FOR HETEROSTRUCTURES

A. PCOR-SIMS^{SM}: SiGe materials

To solve this problem, we at Eurofins EAG Laboratories had to determine, empirically, just how the B sensitivity, as well as

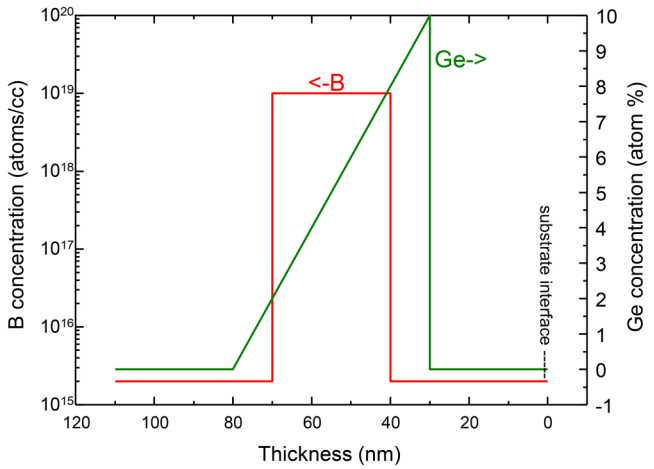

FIG. 2. Design characteristics of a SiGe HBT.

those for the other dopants and impurities, changed with [Ge]. For this, the normal equation for impurity concentration, Eq. (2) above, had to be changed to incorporate a term that adjusted the RSF as a function of [Ge],

$$\rho_i = \frac{I_i}{I_m} \mathrm{RSF} \times f(\mathrm{Ge}), \tag{3}$$

To determine this function, we made implants of B, P, C, and O into SiGe samples with RBS-determined [Ge] of 5%, 10%, 15%, 20%, 24%, 28%, and 45%. The implant doses were calibrated using Si "witness" samples that were implanted along with the SiGe samples. These reference materials were used to generate a series of RSFs over the range of Ge compositions to determine the degree of sensitivity change with [Ge]. Figure 3 shows that the change in B sensitivity is 67% for a [Ge] of 45% with respect to its sensitivity in pure Si.

The blue points on the graph show the error that would occur if [B] is calculated using a Si-based RSF in Eq. (2) (non-PCOR-SIMS^{SM} method). The magenta points on the graph show the error when using the PCOR-SIMS^{SM} method, which uses the measured [Ge] for each data point. Since [Ge] is measured for each impurity data point, it does not have to remain constant throughout the profile, and accurate concentrations can be measured for all depths of the profile.

However, for this correction to be used, one has to be able to determine [Ge] accurately for every data point over the entire range of expected Ge concentrations in a SiGe structure, from 0% atomic to 95% atomic. We developed a way of doing this. It was tested by comparing the results of the SIMS-determined [Ge] in a stairstep structure compared with Auger electron spectrometry (AES)-determined [Ge]. (The accuracy of the AES results was verified previously by Rutherford backscattering spectrometry). The results showed that the SIMS-determined Ge concentrations were

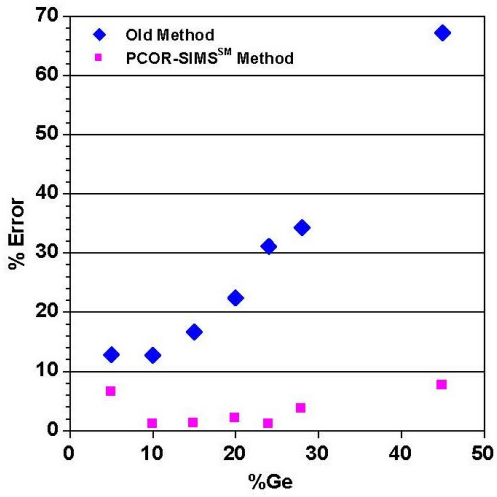

FIG. 3. Error in using B RSF calculated from a Si standard and the error when using PCOR-SIMS^{SM} vs Ge content. The blue diamonds—Si-based RSF "Old method." The magenta squares—PCOR-SIMS^{SM} correction using the measured [Ge] for each data point "New method"[13] [Reprinted with permission from Denker *et al.*, *Proceedings of the 12th International Conference on Secondary Ion Mass Spectrometry.* Copyright 2000, Elsevier.].

accurate within 5% relative over a range of 5–45 at. % Ge [see (A)–(C) of the Data Availability section].

A test of the PCOR-SIMS^{SM} correction for [Ge] is shown in Fig. 4. A boron implant was made into two samples: a SiGe layer of a constant 52% atomic Ge, and one sample of a SiGe layer of a constant 75% atomic Ge deposited on pure Si. The profile into the constant composition SiGe can be considered as the reference profile. For the implant made into the SiGe/Si sample, if Si-based RSF is used throughout, the profile is a factor of 2, too low in the SiGe layer. Using the PCOR-SIMS^{SM} f(Ge) functionality and correction for the measured [Ge] at every data point, the profile matches the reference profile perfectly.

Figure 5 shows an example more commonly found in SiGe transistor fabrication technology. The figure shows a SiGe layer deposited over a pure Si layer with a top layer of pure Si. The figure shows the error in the B profile when using only a Si RSF normalized to the Si matrix profile (green) compared to the profile using the PCOR-SIMS^{SM} data processing protocol (blue). A comparison of the two profiles shows how the B profile is corrected only within the SiGe layer. The profile is unaffected outside of SiGe. These show that the correction procedure is truly point-by-point.

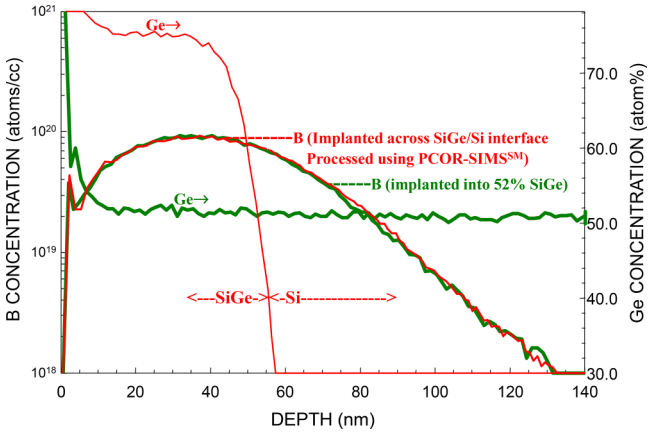

FIG. 4. Shown is a test of the PCOR-SIMS^{SM} function, f(Ge), for B sensitivity in SiGe and pure Si. The B and Ge colors match for each sample. The green curve shows a B implant into SiGe with a constant [Ge] of 52% (reference profile). The red curve shows the PCOR-SIMS^{SM} corrected profile of the same implant made into a SiGe layer of 75% Ge deposited on pure Si.

B. PCOR-SIMS^{SM}: III–V materials

Quantification in III–V compound semiconductor heterostructures is even more difficult because there are many more combinations of dopants and impurities in a much wider array of matrices, most of which come in a wide variety of stoichiometries. This requires a large number of standards because, even though some III–Vs may appear similar, i.e., GaAs and InGaAs, the difference in matrix composition is enough to change the sensitivity of dopants and impurities to a significant degree. This requires one to have more than a hundred standards for just the dopant/impurity matrix combinations found in the modern day III–V materials. But, if we are to achieve accuracies of "better than a factor of 2," these standards are required.

But, the situation is not as intimidating as it sounds if we use sophisticated data processing such as PCOR-SIMS^{SM}. We can use empirical measurements of the effect of stoichiometry on the elemental sensitivities and arrive at a function that corrects the dopant and impurity sensitivities, point-by-point, based on the measured stoichiometry at any given depth in the profile.

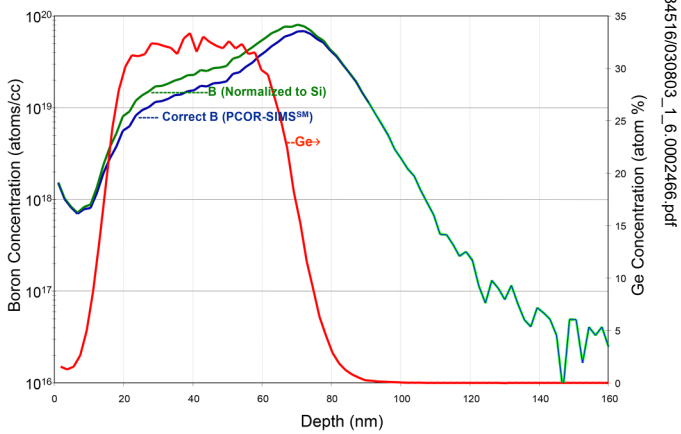

FIG. 5. Boron distributions through the SiGe region of a transistor show the difference between using a Si RSF throughout, i.e., B(Normalized Si) and using a PCOR-SIMS^{SM} correction, i.e., Correct B (PCOR-SIMS).

For example, one of the most challenging structures that we are called upon to measure is the AlGaAs vertical cavity surface emitting laser (VCSEL). A complete SIMS profile of such a device is shown in Fig. 6.[14]

The structure is composed of more than 200 AlGaAs layers with stoichiometries ranging from $Al_{0.07}Ga_{0.93}As$ up to $Al_{0.95}Ga_{0.05}As$. The continuously changing Al composition causes the sensitivities of the dopants and impurities to change with depth. But we can again correct RSFs by empirically determining how the Al concentration, [Al] affects the sensitivity of impurities and dopants and then formulate a function to put into the RSF equation:

$$\rho_i = \frac{I_i}{I_m} \mathrm{RSF} \times f(\mathrm{A1}). \quad (4)$$

This was done by implanting the carbon and silicon dopants (and impurities) into matrices from GaAs to AlAs. We found that, compared to GaAs, the sensitivities increased by a factor of 2 at a stoichiometry of $Al_{0.6}Ga_{0.4}As$, and as much as a factor of 3 at stoichiometries approaching pure AlAs, which are encountered in the aperture layer of the VCSEL structure.[14]

But, as with SiGe, we have to be able to determine the matrix composition, in this case Al, accurately. We did this by measuring Al and Ga profiles in a multilayer AlGaAs structure with compositions ranging from $Al_{0.07}Ga_{0.93}As$ up to $Al_{0.79}Ga_{0.21}As$. The Al concentrations measured by SIMS agree to be within 5% relative of the RBS measurements taken on the same sample.

The effect of using the PCOR-SIMS^{SM} f(Al) correction to sensitivity factors can be seen in Fig. 7. Silicon and carbon were implanted across the $Al_{0.8}Ga_{0.2}As$/GaAs interface. Without the PCOR-SIMS^{SM} correction (using GaAs RSFs), the Si and C concentrations in the $Al_{0.8}Ga_{0.2}As$ layer would be too low by as much as a factor of 2. You can also see how the PCOR function corrects the profiles even at the interface, and how PCOR-SIMS^{SM} has no effect in the underlying GaAs because the [Al] is < 0.003 Group III atom fraction.

This shows the importance of using PCOR-SIMS^{SM} corrected RSFs when plotting C and Si and not relying on GaAs standards for quantification. The accuracy of the dopant concentrations is important because the distributed Bragg reflectors (DBR) layers not only act as the mirrors of internal reflection of the light emitted from the active region but must also serve as the layers from which carriers are injected into the active region. If doping in the DBR is too low, the resistance will be too high for the high-current injection of carriers. If doping is too high, there will be an excessive scattering of carriers in the layers thereby reducing the efficiency of the device. The doping levels determined by SIMS *have* to be correct in order for the grower of the VCSEL wafer to optimize both electrical and optical device performance. If one fails to use the PCOR-SIMS^{SM} correction for the change in sensitivities due to changing [Al], incorrect calibration of C and Si doping in the n-DBR of a VCSEL can lead to a factor-of-2 error (back to the 1970s again!) in the doping concentration in the high [Al] AlGaAs layers of the DBR.

But changing concentrations of the matrix elements within a depth profile can also affect the sputtering rates. It is critically important that the plotted thicknesses of the layers be correct. The optical properties of the DBR layers are dependent not only on the refractive index (Al content) of each layer but also on the thickness of each layer. By sputtering into AlGaAs materials of a wide range of [Al], we determined that increasing the [Al] reduces the sputtering rate. The sputtering rate of $Al_{0.9}Ga_{0.1}As$ is 25% lower than that of pure GaAs. Using a constant sputtering rate for the entire profile derived from a crater depth measurement will introduce a significant error in the plotted layer thicknesses. PCOR-SIMS^{SM} also makes a correction for these sputtering rate differences, again based on the [Al] at every datapoint in the profile, using the following functionalized equation:

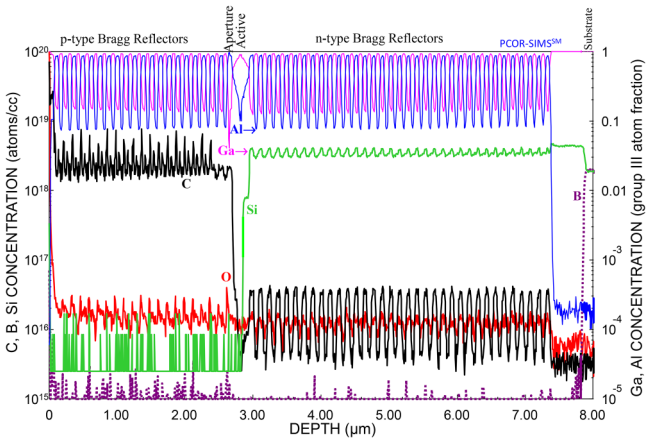

FIG. 6. Shown are both the matrix and dopant profiles in a complete VCSEL structure. All the profiles are acquired in a single analysis. The B profile marks the beginning of the substrate. Reproduced from Buyuklimanli *et al.*, Compd. Semicond. Mag. **20**(3), 45 (2014). Copyright 2014, Angel Business Communications.

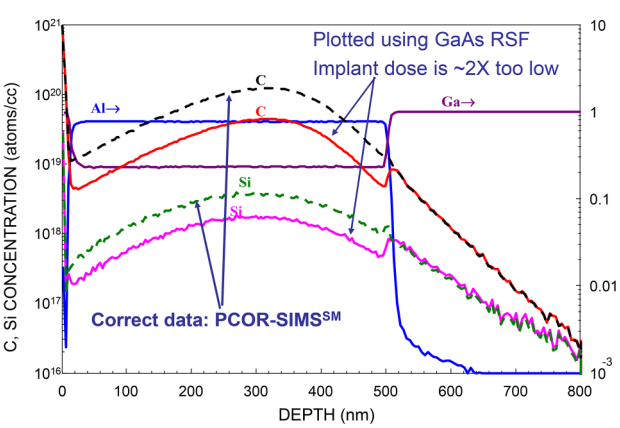

FIG. 7. Graph shows the profiles of Si and C implanted across the Al0.8Ga0.2As/GaAs interface, plotted without the PCOR-SIMS^{SM} correction (solid lines), with the PCOR-SIMS^{SM} correction (dashed curves). The Al and Ga concentrations are plotted in Group III atom fraction along the right-hand axis.

$$D_i = T_i R \times f(Al_i), \quad (5)$$

where D_i is the depth of the data point i, T_i is the sputter time of the data point I, R is the average sputtering rate, and $f(Al_i)$ is a function that corrects R with respect to the [Al] at the data point i. It is easy to understand that without this $f(Al_i)$ PCOR-SIMS^{SM} correction, the plotted thicknesses of all the AlGaAs layers in a VCSEL will be incorrect (too thick).

Another region of the VCSEL structure that must have the layer thicknesses plotted correctly is the active region of the device, shown in Fig. 8.[14] This is where the light is generated. This particular device uses an AlGaAs/GaAs multiquantum well (MQW) active region grown between two "cladding" layers of continuously varying [Al]. The thicknesses of these layers determine, to a large degree, the wavelength of the emitted light that must match the optical characteristics of the DBR layers. Thus, it is critical that the SIMS results provide accurate layer thicknesses to the epitaxial wafer grower. Note that some VCSEL structures use InGaAs for the active layer. We have also determined the effect of [In] on the sputtering rate. Unlike increasing the Al composition, increasing the In composition *increases* the sputtering rate. PCOR-SIMS^{SM} also has a f(In) function to correct InGaAs sputtering rates.

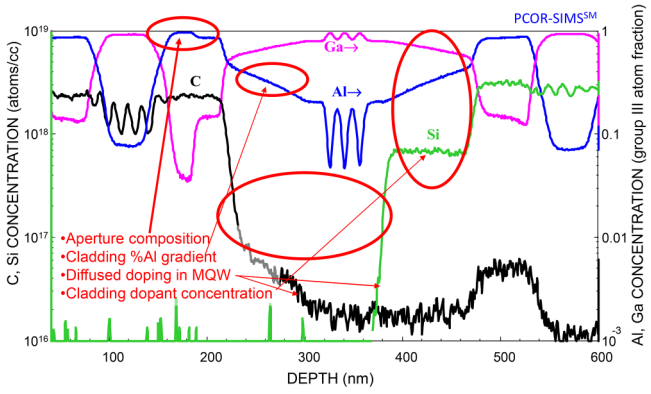

FIG. 8. SIMS profiles in the active region of a VCSEL showing the important regions where accurate concentrations and layer thicknesses are critical. Note that both dopants and matrix elements are measured quantitatively in the same analysis. (Most of the top DBR was removed prior to this analysis in order to obtain a higher layer resolution in this active region.) Reproduced from Buyuklimanli *et al.*, Compd. Semicond. Mag. **20**(3), 45 (2014). Copyright 2014, Angel Business Communications.

C. PCOR-SIMS^{SM}: Boron plasma doping of poly-Si gates

In memory applications, a mask step can be eliminated in the manufacture of CMOS pMOSFETs if the *in situ* doped, n-type poly-Si gates can be counter-doped with B. High doping is required to have acceptable poly depletion at the poly/gate-oxide interface. Plasma doping provides throughput advantages over beamline implantation for this ultra-high-dose application. Very high doses (5×10^{16} to 1×10^{17} atoms/cm^2) are needed. But plasma doping energies cannot be greater than 7 keV in order to ensure gate oxide integrity (for 700 Å poly, lower energy for thinner poly).

Early on, we found that these very high B concentrations (often >50% atomic), changed the B sensitivity. To investigate this effect quantitatively, we had very high-dose B implants made into both Si and SiO_2. Peak B concentrations reached as high as 2×10^{22} atoms/cm^3. We found that a correction to the B RSF was needed for B concentrations $>5 \times 10^{21}$ atoms/cm^3. This was the case for both Si and SiO_2. Using these experimentally developed relationships of B sensitivity vs [B], we devised a function, f(B), and included it in the PCOR-SIMS^{SM} equation for calculating [B] for every B concentration in the profile:

$$\rho_i = \frac{I_i}{I_m} RSF \times f(B). \quad (6)$$

We also found that the high [B] also reduced the sputtering rate for both Si and SiO_2 by as much as 12% in SiO_2 and up to 23% in Si. We then fed these relationships into the PCOR-SIMS^{SM} formulas to correct the measured profiles for both [B] and depth for every data point in the analysis.

To check the effectiveness of these corrections for high B concentrations, we had a series of low-energy, high-dose B implants made in Si to simulate the high doses encountered in plasma doping. We then had them analyzed for boron dose by two different laboratories using nuclear reaction analysis (NRA), a highly precise accelerator-based technique that is free of matrix effects but *does* require a standard. (The standard we used was a B implant into Si with its dose confirmed by measuring it side-by-side with the NIST standard reference material, SRM-2137, of B in Si which has a certified accuracy of ±3%.) We compared the doses of the low-energy, high-dose B implants measured by NRA with the doses measured by SIMS using several experimental protocols, including PCOR-SIMS^{SM}. Since the integrated dose of the SIMS profile is affected by both the concentration and depth scale accuracies, this experiment tests the accuracy of *both* PCOR-SIMS^{SM} correction functions.

The average of the two NRA datasets over a B dose range of 5×10^{13} atoms/cm^3 to 4×10^{15} had a correlation coefficient better than 0.95 with an absolute accuracy near that of the NIST SRM used for calibration. As expected, no deviation from linearity was observed even at the highest B doses and concentrations (2.6×10^{22} atoms/cm^3).

SIMS was performed on the same wafers using three different protocols. The first used 1 keV O_2^+ bombardment at 60° with respect to the surface normal while using oxygen flooding (O-leak) to stabilize ion yields near the sample surface. This was a standard protocol used by many laboratories in the early 2000s. A second protocol used 700 eV O_2^+ bombardment at 45° with oxygen flooding, which was also used at that time. While both of these protocols were in good agreement with the NRA results at lower doses and lower concentrations, they both deviated significantly for doses of 2×10^{15} atoms/cm^2 and above. The error at 3.2×10^{15} atoms/cm^2 (2.5×10^{22} atoms/cm^3) was 20%. This was clearly unacceptable for plasma doping of poly gates which used doses even higher than those used in this study.

The third protocol used the same bombarding conditions as the first protocol but without using oxygen flooding but *with*

PCOR-SIMS^{SM} for the data processing. These results were virtually identical to the NRA results up to and including a dose of 2×10^{15} atoms/cm^2 and were within 4% of the NRA results at a B dose of 3.2×10^{15} atoms/cm^2. These results were proof that the experimentally determined functions for correcting B sensitivity and sputtering rate for these types of Si samples with very high [B] resulted in significantly more accurate B profiles than did the protocols that did not account for the effect of [B] on B sensitivity and the sputtering rate.

However, the real test was to see how well the PCOR-SIMS^{SM} method of quantification worked on a real plasma-doped poly-Si gate sample. Figure 9 shows the results of PCOR-SIMS^{SM} analysis (blue) and XPS analysis (red) overlaid on a bright field STEM image of a poly-Si gate structure that has been plasma-doped with B at 7 keV to a dose of 1×10^{17} atoms/cm^3.

The contrast difference in the STEM image between the poly-Si and Si substrate shows that the extremely high dose of the plasma implant changed the morphology and reduced the average mass of the poly-Si layer. However, you can also see a region within the implanted zone that is still lighter, which coincides with the region of the highest B concentration near the surface detected in the PCOR-SIMS^{SM} data. The PCOR-SIMS^{SM} profile also shows a peak of oxygen in the middle of the B-implanted zone where a contrast change is observed in the STEM image. Curiously, the B profile shows a decrease that corresponds to the peak in the oxygen profile. To verify these features observed in the PCOR-SIMS^{SM} and STEM data, we acquired XPS profiles. As can be seen by the red curve in Fig. 9, both the dip in B and the peak in oxygen were confirmed by XPS. It is difficult to compare B concentrations determined by these two techniques as the conversion of atoms/cc to atom % is not trivial in such a complex composition. The B peak-to-valley range difference between PCOR-SIMS^{SM} and XPS data can be attributed to the depth resolution difference in these two techniques. Note also that the depth scale of PCOR-SIMS^{SM} analysis matched the STEM image showing that the sputter rate correction function resulted in the correct depth scale despite the lower sputtering rate within the highly boron-doped region of poly-Si. The source of the O peak in the middle of the B-implanted region is unknown. It should also be pointed out that the oxygen profile by SIMS reaches a steady state in poly-Si because oxygen was used for sputtering in SIMS analysis.

Perhaps. most importantly, the accuracy of the B quantification of PCOR-SIMS^{SM} analysis is shown in the B doses measured by NRA and SIMS, shown near the top of the figure. The agreement of 3.5% between the two techniques is remarkable considering the fact that the maximum [B] of 5×10^{22} atoms/cm^3 is nearly half of the atomic density of pure elemental B (1.3×10^{23} atoms/cm^3). This shows that the f(B) function in Eq. (6) is effective at correcting even large differences in sensitivity and sputtering rate encountered in these plasma-doped samples.

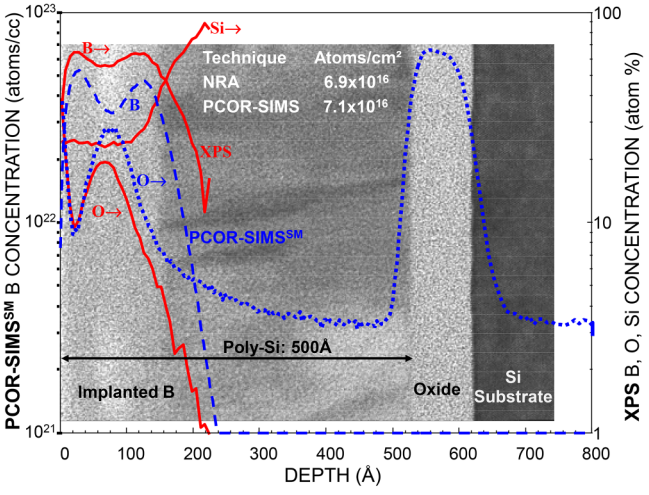

FIG. 9. Shown is an overlay of PCOR-SIMS^{SM} analysis (blue) and XPS analysis (red) onto a bright field STEM image of a poly-Si gate structure that has been plasma-doped with B at 7 keV to a dose of 1×10^{17} atoms/cm^3. NRA determined, and PCOR-SIMS^{SM} determined doses are also shown in the figure. They agree to be within 3.5%. [Oxygen profile by SIMS (blue) is nonquantitative].

IV. SUMMARY AND CONCLUSIONS

SIMS started out in 1958 with no ability to do quantitative analysis, and indeed, with little hope of doing so. But, a decade later, people were able to use thermodynamics to predict elemental sensitivities with accuracies within a factor of 2 for silicate matrices. (Despite this sample restriction, this LTE approach worked well enough for one of the first applications of SIMS – that of analyzing grains in Moon Rocks in 1969). In the late 1970s, SIMS started to be used for semiconductors, with the first methodology, published in 1980, for using ion-implanted materials as SIMS standards for semiconductors. The use of ion-implanted materials as standards for determining sensitivity factors continued for another 15 years, until the need arose for accurate quantification in samples, in which, the matrix changed with depth (heterostructures). It soon became apparent that using different sensitivity factors in different layers would no longer be practical because of the graded layer compositions and the enormous number of matrix stoichiometries that were becoming commonplace in Si-based and III–V semiconductor structures. In the late 1990s to early 2000s, PCOR-SIMS^{SM} was developed by Eurofins EAG Laboratories to solve these seemingly intractable quantification problems.

ACKNOWLEDGMENTS

Charles Magee, wishes to make posthumous acknowledgment to his first supervisor, Richard Honig, of RCA laboratories, for starting him on this wonderful road to SIMS and for guiding us all with this seminal publication in 1958, *The Application of Mass Spectrometry to the Study of Surfaces by Sputtering*, Ref. 1.

AUTHOR DECLARATIONS

Conflict of Interest

The authors have no conflicts to disclose.

Author Contributions

Charles W. Magee: Conceptualization (equal); Writing – original draft (equal); Writing – review & editing (equal). **Temel H. Buyuklimanli:** Conceptualization (equal); Data curation (equal); Software (equal); Writing – review & editing (equal).

DATA AVAILABILITY

The data that support the findings of this study are openly available in Science and Technology of Materials, Interfacing, and Processes at https://avssymposium.org/AVS1998/Sessions/Schedule/64325, Ref. 15; Eurofins EAG at https://www.eag.com/wp-content/uploads/2017/05/M-024717-article-compound-semiconductor-scrutinizing-VCSELs-by-SIMS-may2014rev.pdf, Ref. 16; and Eurofins EAG at https://www.eag.com/wp-content/uploads/2020/10/M-051520_Understanding-VCSELs.w.pdf, Ref. 17.

REFERENCES

[1]R. E. Honig, J. Appl. Phys. **29**, 549 (1958).
[2]R. E. Honig, in *Advances in Mass Spectrometry*, edited by J. D. Waldron (Pergamon, London, 1959), pp. 162–171.
[3]C. A. Andersen, Int. J. Mass Spectrom. Ion Phys. **2**, 61 (1969).
[4]V. E. Krohn, J. Appl. Phys. **33**, 3523 (1962).
[5]C. A. Andersen, Int. J. Mass Spectrom. Ion Phys. **3**, 413 (1970).
[6]C. A. Andersen and J. R. Hinthorne, Anal. Chem. **45**, 1421 (1973).
[7]C. A. Andersen, in *NBS Special Publication SP-427*, edited by K. F. J. Heinrich, D. E. Newbury (US Dept. of Commerce, Washington, D.C, 1975), p. 79.
[8]D. E. Newbury, in *Quantitative Surface Analysis of Materials, STP 643*, edited by N. S. McIntyre [American Society for Testing and Materials (ASTM), Philadelphia, PA, 1978], p. 127.
[9]H. A. Storms, K. F. Brown, and J. D. Stein, Anal. Chem. **49**, 2023 (1977).
[10]W. H. Hofker, D. P. Oosthoek, N. J. Koeman, and H. A. M. De Grefte, Radiat. Eff. **24**, 223 (1975).
[11]D. P. Leta, G. H. Morrison, G. L. Harris, and C. A. Lee, Int. J. Mass Spectrom. Ion Phys. **34**, 147 (1980).
[12]D. P. Leta and G. H. Morrison, Anal. Chem. **52**, 514 (1980).
[13]M. S. Denker, T. H. Buyuklimanli, and J. T. Mayer, in *Proceedings of the 12th International Conference on Secondary Ion Mass Spectrometry*, edited by A. Benninghoven, P. Bertrand, N. H. Migeon, H. W. Werner (Elsevier Science B.V., Amsterdam, 2000), p. 639.
[14]T. Buyuklimanli, C. W. Magee, J. Serfass, and J. Kipnis, Compd. Semicond. Mag. **20**, 45 (2014).
[15]B. R. Rogers, R. Gregory, G. Harris, D. Werho, W. Chen (1998). Application of Surface Analysis Techniques to Semiconductor Technology, AVS https://avssymposium.org/AVS1998/Sessions/Schedule/64325
[16]T. Buyukumanu, C. Magee, J. Serfass, and J. Kipns (2014). VCSELs by SIMS, Compound Semiconductor, https://www.eag.com/wp-content/uploads/2017/05/M-024717-article-compound-semiconductor-scrutinizing-VCSELs-by-SIMS-may2014rev.pdf
[17]C. Magee, M. Salmon, and T. Buyuklimanli (2020). Understanding VCSELs: From epitaxial wafer growth to failure analysis, eurofins, https://www.eag.com/wp-content/uploads/2020/10/M-051520_Understanding-VCSELs.w.pdf